

First detection of phase-dependent colliding wind X-ray emission outside the Milky Way¹

Yaël Nazé²

Institut d'Astrophysique et de Géophysique, Université de Liège, Allée du 6 Août 17, Bat. B5c, B4000 - Liège (Belgium)
naze@astro.ulg.ac.be

Michael F. Corcoran

Universities Space Research Association, 7501 Forbes Blvd, Ste 206, Seabrook, MD 20706, and Laboratory for High Energy Astrophysics, Goddard Space Flight Center, Greenbelt, MD 20771 (USA)
corcoran@milkyway.gsfc.nasa.gov

Gloria Koenigsberger

Instituto de Ciencias Fisicas, Universidad Nacional Autónoma de México, Apartado Postal 48-3, Cuernavaca, Morelos 62251, Mexico
gloria@astroscu.unam.mx
and

Anthony F.J. Moffat

Département de Physique, Université de Montréal, CP 6128, Succursale Centre-Ville, Montréal, QC H3C 3J7, and Observatoire du Mont Mégantic, Canada
moffat@ASTRO.UMontreal.CA

ABSTRACT

After having reported the detection of X-rays emitted by the peculiar system HD 5980, we assess here the origin of this high-energy emission from additional X-ray observations obtained with XMM-Newton. This research provides the first detection of apparently periodic X-ray emission from hot gas produced by the collision of winds in an evolved massive binary outside the Milky Way. It also provides the first X-ray monitoring of a Luminous Blue Variable only years after its eruption and shows that the source of the X-rays is not associated with the ejecta.

Subject headings: stars: individual (HD 5980) – stars: Wolf-Rayet – stars: winds – Magellanic Clouds – X-rays: binaries

²Postdoctoral Researcher F.N.R.S.

¹Based on observations collected with XMM-Newton, an ESA Science Mission with instruments and contributions directly funded by ESA Member States and the USA (NASA).

1. Introduction

The most massive stars, which are also the most luminous (and for most of their lives the hottest) stellar objects, have a large impact on their host galaxies. For example, throughout their evolution, these stars convert simple into more complex ele-

ments, and distribute them into space by a complex process of mass loss. They are thus largely responsible for the chemical enrichment of the Universe (Massey 2003). Their intense, hot photon emission is also able to ionize the surrounding medium (leading to the formation of HII regions) and to drive a continuous ejection of matter in the form of a stellar wind. Finally, massive stars inject a large amount of mechanical energy into their host galaxies, through e.g. supersonic winds, large transient eruptions (like those of Luminous Blue Variables, e.g. η Carinae), or GRB/supernova explosions (Massey 2003).

In massive early-type binaries, the supersonic outflow from one star collides with that of its companion. This collision provokes a strong heating of the shocked wind, leading to the emission of X-rays (see e.g. Stevens et al. 1992). Hints of this high-energy phenomenon were already found two decades ago, when the first X-ray observatories detected overluminosities in hot binaries (Pollock 1987; Chlebowski & Garmany 1991). However, since additional X-ray emission can have several origins, not restricted to colliding winds (CW), indisputable observational evidence of CW X-ray emission had to await the advent of a new generation of sensitive X-ray facilities (Chandra, XMM-Newton). Indeed, only detailed spectroscopic investigations and careful monitoring in the X-rays can bring to light the actual properties of the hot gas produced by the wind-wind collision. Most notably, phase-locked variations in the X-ray domain are produced by varying separation in eccentric binaries (that changes the intrinsic strength of the collision) or varying line-of-sight opacity as the stars revolve around each other: see e.g. HD 152248 (Sana et al. 2004), HD 93403 (Rauw et al. 2002), WR 25 (Pollock & Corcoran 2006), and γ^2 Vel (Schild et al. 2004). Up to now, all studied X-ray colliding wind (XCW) systems belong to our Galaxy - a few XCW candidates have been proposed in 30 Doradus, but solely on the basis of an X-ray overluminosity (Portegies Zwart et al. 2002), which is insufficient to ascertain their nature. Studying the CW phenomenon in other galaxies can provide an important probe of the mass-loss process in different environments with different metallicities.

HD 5980, the most peculiar massive star in the Small Magellanic Cloud (SMC), lies on the periph-

ery of the large cluster NGC 346 associated with the giant HII region N66. It is a multiple system whose main component, star A, underwent two LBV-like eruptions in 1993-1994, increasing its brightness by up to 3 magnitudes (Jones & Sterken 1997). Together with star B, believed to be an early Wolf-Rayet star of the nitrogen sequence, it forms a close eclipsing binary system whose period is 19.3d, eccentricity is 0.3 and inclination very close to 90° (Sterken & Breysacher 1997). Using the ephemeris of the latter authors, Star A (resp. B) eclipses its companion at $\phi=0$ (resp. 0.36), whereas periastron and apastron occur at phases 0.09 and 0.59, respectively. A third stellar object, star C (probably an early O-type star), contaminates the light of the system, but it is still unclear if this star is just a line-of-sight coincidence or an object gravitationally bound to the close AB pair. The presence of an additional component (e.g. a close orbiting neutron star) has been proposed, based on a 7-hour periodicity seen in spectral and photometric variations and stochastic polarimetry changes, but is still debated (see e.g. Villar-Sbaffi et al. 2003). Moffat et al. (1998) infer the presence of a wind-wind collision region in the AB system on the basis of strong emission-line variability. From UV observations, Koenigsberger et al. (2000) and Koenigsberger (2004) conclude that the orientation of the shock cone is such that it wraps around Star B, consistent with the notion that Star A possesses the more powerful of the two winds.

The detection of X-ray emission from HD 5980 was reported for the first time by Nazé et al. (2002). Variations of the X-ray brightness were detected, in the short-term range (Nazé et al. 2002) as well as the long-term range (Nazé et al. 2004). However, these observations were not sufficient to determine the nature of these variations (e.g. variations driven by changes in the shocked ejecta from the 1994 eruption, or phase-dependent changes due to wind-wind collisions in the AB binary), and the origin of the X-ray emission therefore remained uncertain. To resolve this, we requested additional monitoring of HD 5980 with XMM-Newton.

This letter is organized as follows. Section 2 describes the observations while Sections 3 and 4 present the results of the dedicated XMM-Newton campaign and their interpretation, respectively.

Section 5 give our conclusions.

2. Observations and Data Reduction

During the past years, HD 5980 was observed once with Chandra during 100 ks and five times² with XMM-Newton for approximately 20 ks each time (see Table 1). For the latter observations, the three European Photon Imaging Cameras (EPICs) were operated in the standard, full-frame mode (except for the first pn dataset) and a medium filter was used to reject optical light. Note that the observations were carefully planned to sample crucial phases of the 19.3d orbit (Fig. 1); moreover, the last three observations were obtained during the same 19.3d orbit of HD 5980. To ensure a coherent reduction, we used the Science Analysis System (SAS) software, version 7.0, to re-process all X-ray data. After the pipeline chains, filters recommended by the SAS team were applied in order to keep only the best data (see e.g. Nazé et al. 2006). For consistency, no additional temporal filtering was done.

To each XMM-Newton dataset, we applied the SAS source detection algorithm (*edetect.chain*) in a region of 150" radius around HD 5980, in order to derive the best value of the centroid of the X-ray emission. Since HD 5980 appears surrounded by a soft, X-ray bright SuperNova Remnant (SNR, see Nazé et al. 2002), the detection was restricted to the 1.5–10. keV range, to minimize the contamination from this soft extended source. As a check, we compared these results with the output of another algorithm (SAS task *eregionanalyse*) that simply calculates the number of counts in the region considered³ and corrects them only for the Encircled Energy Fraction (about 0.8 in our case). Within the error bars, both methods agree with each other so we only present the results from the latter (see Table 1).

²A sixth observation taken during Rev. 0970 was strongly affected by a flare, rendering the data unusable.

³We used a 25" region centered on HD 5980, together with a background region of the same area but offset from HD 5980 by 22s east in RA (or -2040 px in X) and 82" south in DEC (or -1640 px in Y). Using an annular background region yields the same results, though noisier.

3. Results

It must first be noted that two XMM-Newton datasets were taken, intentionally, at the same phase ($\phi \sim 0.36$). Although these two observations were obtained during XMM-Newton Revs. 0157 (2000 Oct.) and 1094 (2005 Nov.), i.e. separated by 5 years or 97 orbital revolutions of the AB system, they present very similar values for the count rate of HD 5980 (Fig. 2 and Table 1). This means that post-eruption, epoch-dependent variations are minimal. Indeed, if a significant part of the X-ray emission came from the collision of the fast wind with the slower ejecta associated with the 1994 eruption, a monotonic decrease in the X-ray brightness and a decline in the X-ray temperature with time would be expected as this interaction zone expands and cools.

Second, coherent variations with phase are now clearly detected, with X-ray emission steadily increasing towards $\phi = 0.36$ (Figs. 2 and 3). At that time, the emission also appears slightly harder, though we cannot exclude a constant value of the HR at the 2σ level. This bright phase corresponds to the eclipse of Star A by its companion, i.e. when the opening of the shock cone, slightly concave with respect to Star B, is directed towards the observer (Fig. 1).

Although we cannot compare directly the Chandra and XMM-Newton count rates (because of background contamination, different spatial resolution, and cross-calibration problems), it must be noted that the variations measured by Chandra confirm the trend seen by XMM-Newton. During the 100 ks of the Chandra observation, the count rate clearly increased from 2 to 4×10^{-3} ctss⁻¹ in the 0.3–10. keV band (Nazé et al. 2002) or from 1 to 2×10^{-3} ctss⁻¹ in the 1.5–10. keV band (Fig. 2). These data covered phases ranging from 0.24 to 0.30. In this interval, the XMM-Newton lightcurve indeed predicts an increase of $\sim 1 \times 10^{-3}$ ctss⁻¹ in the count rate.

Finally, we investigated the X-ray spectrum of HD 5980. Of course, the faintness of this distant source and the contamination at low energies by the superposed SNR prohibit any detailed study. However, since the spectral properties of the SNR contamination can be determined thanks to the high-resolution Chandra data of Nazé et al. (2002), a first, general spectral evaluation can be

made: our data only reveal a clear, usable excess at high energies for Revs. 0157, 1093 and 1094 (i.e. when HD 5980 is the brightest). This high-energy emission was fitted by an absorbed optically-thin plasma model (mekal, in Xspec v11.2.0): compared to the spectral properties reported by Nazé et al. (2002), only changes of the flux level were detected; within the confidence intervals, the absorption and temperature do not seem to vary in a significant way. However, it must be noted that the spectra are rather noisy and that only large variations would be detected.

4. Discussion

The observed variations of the X-ray emission from HD 5980 can be qualitatively explained by considering the geometry of the CW region in the close A+B binary.

The change in the X-ray flux could be related to absorption. Indeed, at phases close to 0.36, the opening of the shock cone is directed towards the observer and the X-ray emission of the CW region is thus seen through the lower density wind of Star B (Koenigsberger 2004 and Fig. 1). The lower absorption results in an increase of the observed X-ray luminosity. At other phases, the very dense, slower wind of star A strongly absorbs at least part of the CW emission; the width of the lightcurve is then directly related to the opening angle of the shock cone. Such a scenario has been proposed to explain the behaviour of the WR+O binary γ^2 Vel (Schild et al. 2004).

However, the available observations do not yet enable us to ascertain that the maximum brightness really occurs at/near $\phi=0.36$. For example, it is conceivable that the count rate actually continues to increase beyond this phase, e.g. to peak at apastron. A similar variation, proportional to the separation between the stars rather than inversely proportional, was observed for Cyg OB2 #8A (De Becker et al. 2006). In that case, the variation was explained by a sudden decrease of the wind velocity at periastron because of a strong radiative inhibition/braking or as a result of perturbations associated with tidal bulge interactions. For HD 5980, such changes of the wind velocity would mean that the X-ray emission should not only be stronger, but also harder towards apastron, as suggested by the available data.

To distinguish between these two scenarios, additional X-ray observations are necessary in order to complete the lightcurve near apastron. This would enable us to notably determine the position of the brightness peak (apastron or eclipse of A by B ?) and the exact shape of this increase. A detailed spectral analysis is also needed, but it requires better spatial resolution than that of XMM-Newton in order to cleanly disentangle HD 5980 from the superposed SNR, therefore permitting access to the lower energy range which is more affected by the absorption variations.

In addition, hydrodynamical modelling of the fast wind/slow wind interaction region and the CW area should be undertaken to quantify their respective strength and expected modulation. In this context, the lack of strong secular variations over 5 years is rather puzzling, since, during this interval, the wind density of Star A changed, as witnessed in the UV and optical emission lines (Koenigsberger 2004). However, the X-ray luminosity (in the radiative limit) goes as $L_X \propto \dot{M} \times v_\infty^2$ (Stevens et al. 1992), and since the eruption the terminal velocity of the wind of star A has increased from about 600 km s⁻¹ to about 2000 km s⁻¹ (Koenigsberger 2004), which offsets the order-of-magnitude decline in the mass loss rate over that interval. On the other hand, the relative constancy of the X-ray brightness at $\phi = 0.36$ despite a significant decline in the mass loss from Star A might indicate that Star A's wind has mainly changed in the direction perpendicular to the orbital plane than it has in the orbital plane, as might be expected if the mass loss from star A is not spherically symmetric (Villar-Sbaffi et al. 2003, (i.e. bipolar - see). Note however that the observed P-Cygni UV absorption lines indicate that at least some of Star A's wind variation occurred near the orbital plane (Koenigsberger 2004, and references therein).

5. Summary and Conclusions

An XMM-Newton monitoring campaign of the peculiar massive binary HD 5980 has unveiled the variations of its X-ray emission. As two observations taken 5 years apart (a separation of more than 90 binary orbits!) present similar count rates, the main source of X-rays cannot be the fast wind/slow wind interaction following the LBV-like

eruption of Star A, since its emission is expected to monotonically and rapidly decrease with time. Because individual Wolf-Rayet stars and LBVs are only weak X-ray sources, the high-energy radiation must be associated with the wind-wind collision in the close A+B pair, a fact further supported by the detection of phase-dependent changes. This is the first time that the presence of X-ray emitting gas produced by the collision of winds in a binary has been confirmed outside our Galaxy.

The X-ray emission of HD 5980 appears modulated with phase: a clear increase is observed towards the time of the eclipse of Star A by its companion. This can be due either to the lower absorption inside the shock cone (a situation reminiscent to that of γ^2 Vel) or to a lower wind velocity at periastron (similar to the behaviour of Cyg OB2 #8A). Additional data and hydrodynamical modelling are now needed to further distinguish between these two scenarios.

YN acknowledges support from the Fonds National de la Recherche Scientifique (Belgium), the PRODEX XMM and Integral contracts, and the visitor's program of the GSFC. GK acknowledges support from DGAPA/PAPIIT IN 119205. AFJM is grateful for financial support from NSERC (Canada) and FQRNT (Quebec).

Facilities: XMM-Newton (EPIC), CXO (ACIS).

REFERENCES

- Cantó, J., Raga, A., & Wilkin, F.P. 1996, *ApJ*, 469, 729
- Chlebowski, T., & Garmany, C.D. 1991, *ApJ*, 368, 241
- De Becker, M., Rauw, G., Sana, H., Pollock, A.M.T., Pittard, J.M., Blomme, R., Stevens, I.R., & van Loo, S. 2006, *MNRAS*, 371, 1280
- Koenigsberger, G. 2004, *RMxAA*, 40, 107
- Koenigsberger, G., Georgiev, L., Barbá, R., Tzvetanov, Z., Walborn, N.R., Niemela, V., Morrell, N., & Schulte-Ladbeck, R., 2000, *ApJ*, 542, 428
- Koenigsberger, G., Fullerton, A., Massa, A., & Auer, L.H. 2006, *AJ*, 132, 1527
- Jones, A.F. & Sterken, C. 1997, *Astronomical Data* 3, 4
- Massey, P. 2003, *ARA&A*, 41, 15
- Moffat, A.F.J., Marchenko, S.V., Bartzakos, P., Niemela, V.S., Cerruti, M.A., Magalhaes, A.M., Balona, L., St-Louis, N., Seggewiss, W., & Lamontagne, R. 1998, *ApJ*, 497, 896
- Nazé, Y., Hartwell, J.M., Stevens, I.R., Corcoran, M.F., Chu, Y.-H., Koenigsberger, G., Moffat, A.F.J., & Niemela, V.S. 2002, *ApJ*, 580, 225
- Nazé, Y., Manfroid, J., Stevens, I.R., Corcoran, M.F., & Flores, A. 2004, *ApJ*, 608, 208
- Nazé, Y., Rauw, G., Pollock, A.M.T., Walborn, N.R., & Howarth, I.D. 2006, *MNRAS*, submitted
- Pollock, A.M.T. 1987, *ApJ*, 320, 283
- Pollock, A.M.T., & Corcoran, M.F. 2006, *A&A*, 445, 1093
- Portegies Zwart, S.F., Pooley, D., & Lewin, W.H.G. 2002, *ApJ*, 574, 762
- Rauw, G., Vreux, J.-M., Stevens, I.R., Gosset, E., Sana, H., Jamar, C., & Mason, K.O. 2002, *A&A*, 388, 552
- Sana, H., Stevens, I.R., Gosset, E., Rauw, G., & Vreux, J.-M. 2004, *MNRAS*, 350, 809
- Schild, H., Güdel, M., Mewe, R., Schmutz, W., Raassen, A.J.J., Audard, M., Dumm, T., van der Hucht, K.A., Leutenegger, M.A., & Skinner, S.L. 2004, *A&A*, 422, 177
- Sterken, C., & Breysacher, J. 1997, *A&A*, 328, 269
- Stevens, I.R., Blondin, J.M., & Pollock, A.M.T. 1992, *ApJ*, 386, 265
- Villar-Sbaffi, A., Moffat, A.F.J., & St-Louis, N. 2003, *ApJ*, 590, 483

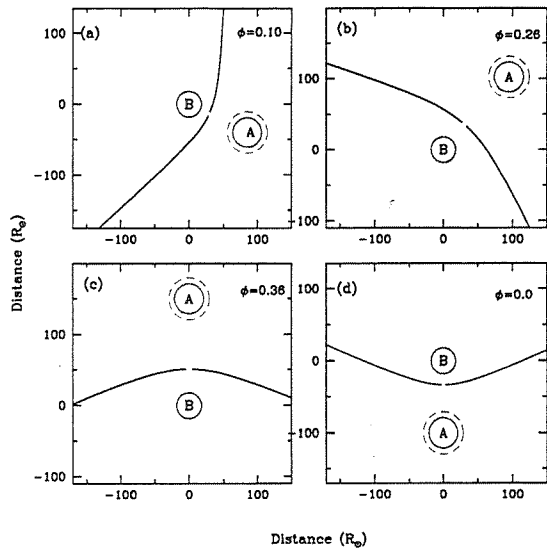


Fig. 1.— Representation of geometry of HD 5980’s wind-wind collision region at the 4 orbital phases for which XMM-*Newton* data are available. The shape of the shock surfaces was computed under the thin shock approximation (Cantó et al. 1996) and assuming that $\dot{M}_A = 1 \times 10^{-4} M_\odot \text{ yr}^{-1}$, $\dot{M}_B = 2 \times 10^{-5} M_\odot \text{ yr}^{-1}$, $v_\infty(A) = 2000 \text{ km s}^{-1}$, and $v_\infty(B) = 2600 \text{ km s}^{-1}$. The broken circle around star A represents the extent of the wind accelerating region (Koenigsberger et al. 2006).

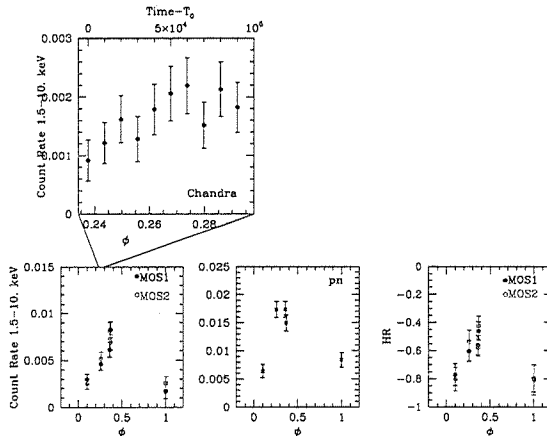


Fig. 2.— Bottom: Evolution of the count rates and hardness ratios with phase from XMM-*Newton* observations (see definitions in Table 1). Top: Count rate of HD 5980 measured during the 100 ks Chandra observation, in the same energy band.

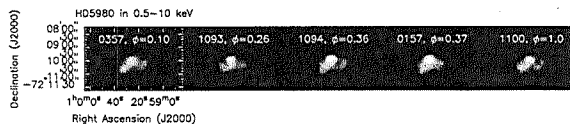


Fig. 3.— Combined MOS images of the area surrounding HD 5980 in the 0.5–10. keV energy range. The data have been binned to get pixels of $2.5''$ and then smoothed with a gaussian of $\sigma = 3\text{px}$.

Table 1: Results from the XMM-*Newton* observing campaign. Count rates were evaluated by the simple *eregionalyse* task and are given in the 1.5-10. keV band (in units of 10^{-3} cts s^{-1}). Hardness Ratios (HR) are defined as $(H - M)/(H + M)$ with M and H the count rates in the 1-2 and 2-10 keV bands, respectively. Phases refer to the ephemeris of Sterken & Breysacher (1997), while dates are Julian Dates minus 2 450 000d.

Rev.	Date	Duration	ϕ	Count rate MOS1	Count rate MOS2	Count rate pn	HR (MOS1)
0157	1835.245	0.245d	0.37	8.26 \pm 0.85	6.95 \pm 0.79	14.92 \pm 1.47	-0.46 \pm 0.06
0357	2234.643	0.322d	0.10	3.00 \pm 0.54	2.54 \pm 0.60	6.41 \pm 1.16	-0.77 \pm 0.08
1093	3701.863	0.218d	0.26	4.64 \pm 0.67	5.16 \pm 0.75	17.32 \pm 1.44	-0.60 \pm 0.07
1094	3703.807	0.207d	0.36	6.13 \pm 0.80	8.14 \pm 0.88	17.41 \pm 1.45	-0.56 \pm 0.07
1100	3716.125	0.208d	1.00	1.70 \pm 0.73	2.60 \pm 0.69	8.38 \pm 1.29	-0.80 \pm 0.10